

Linear and nonlinear numerical wave generation in viscous fluid

Zouhaier Hafsia ⁽¹⁾, Mehdi Ben Haj ⁽²⁾, Hedi Lamloumi ⁽³⁾, Khelifa Maalel ⁽⁴⁾ and Ridha Zgolli ⁽⁵⁾

⁽¹⁻⁵⁾ *ENIT. Laboratoire d'Hydraulique B.P. 37. Le Belvédère, 1002 Tunis, Tunisia*

E-mail : Zouhaier.Hafsia@enit.rnu.tn

Abstract

The proposed two-dimensional (2-D) numerical wave model in the vertical plane is based essentially on two added source terms for the mass conservation and the momentum transport equations. The expression of the mass source term depends on the specified generated wave such as linear monochromatic wave and nonlinear solitary wave. This source term is added for the equation of mass conservation in the internal flow region. To reduce wave amplitude at the end of the active domain, a friction force term is added to the vertical velocity component. An absorption function, decreasing linearly in the horizontal direction, is applied to avoid wave reflection at outlet boundary. The free surface evolution is calculated in terms of Volume Of Fluid (VOF) fraction representative of the cell occupied by the fluid. The convective equation describing the fluid fraction is modified to take into account the non-zero divergence mass conservation equation.

The proposed model is implemented in the PHOENICS code (Parabolic Hyperbolic Or Elliptic Numerical Integration Code Series). For small amplitude wave, propagating on constant water depth, the comparison of numerical and analytical results showed that the free surface and vertical distribution of the velocity components are accurately predicted. For solitary wave, the proposed model generates the free surface profiles induced by this wave correctly with small discrepancy in the tailing edge of the wave. The propagation of the solitary wave in constant water depth indicated that the wave preserved its permanent form and the same wave velocity.

1- Introduction

In laboratory, wave tank has been widely applied to study coastal structures, beach profiles, and other related coastal phenomena. Nowadays, an alternative to physical modeling at laboratory scale is the development of numerical wave tank. Within the numerical model it is easy to test various wave conditions compared to the rebuilding of physical models.

For inviscid fluid, the Laplace equation and the nonlinear free surface boundary conditions are usually solved numerically, using the boundary element method to investigate shoaling of solitary waves up to overturning (Grilli and al., 2001). For most of coastal engineering applications, the Boussinesq equations is used when vertical variation is assumed negligible. This model assumes that the wave amplitude is small enough to ignore the wave dissipation effects by wave breaking (Wei and al., 1999).

To take into account linear or nonlinear water wave propagation with energy dissipation, the Navier-Stokes equations is used. In this model, internal wave generation methods have been widely used to simulate the wave propagation in two dimensions (Lin and al., 1999). This internal wave generation is subdivided in line source and source function methods and permits to avoid the interference with the wave boundary.

The line source method generates waves at a single point along the wave propagation direction. In this method, waves are generated at both sides of the source point by adding, at each time step, to the water surface elevation the corresponding values that are computed by the model equations. Larsen and al. (1983) was the first who used the line source method in

the Boussinesq equations and suggest that the phase velocity is appropriate for the water mass transport.

Madsen and Larsen (1987) were the pioneers to use source function, for wave generation, in the Laplace equation. This method requires several grids to overcome the discontinuity of the source at the wave generation line. This method employs a source term added to the governing equations, either in the form of a mass source in the continuity equation or an applied pressure forcing in the momentum equations (Wei and al., 1999). Based on internal source added to the Navier-Stokes equations model, Kawasaki and al. (1999) show that the non-linear wave generator can be used to study breaking over submerged breakwater.

The waves can also be generated using a wave-maker, which is modeled by a moving object. The wave-maker displacement is determined according to the wave-maker theory (Dong et al., 2001). Another elementary generation method is to impose at the upstream boundary the free surface elevation and the velocity components corresponding to the desired generated wave (Lin and al., 1998).

To prevent the propagation of the wave toward open boundary, the common methods are the use of a radiation condition, with active or passive wave absorbers. Another type of dissipation zone is based on an extra damping pressure added to the free surface, which opposes to the vertical wave velocity. A disadvantage of such damping zones is the increase of the number of computational cells to cover the zone added to the initial domain. Especially, in three dimension models, many computational cells have to be added outside the real computational domain, Kawasaki and al. (1999).

This study will focus on two dimensions numerical linear and nonlinear waves generation in viscous water tanks. The numerical results are compared to analytical solutions describing the symmetric and asymmetric behavior of linear and nonlinear waves. The proposed model is integrated in the Navier-Stokes solver : the PHOENICS code. After validation of the generation method in simple cases, the extension of this method in three dimension and the investigation of wave structure interaction are straightforward.

2- Governing Equations and Boundaries Conditions

2-1 Transport Equations

To generate numerically a given wave, a mass source function is required for the mass conservation equation. In two dimensional, incompressible unsteady flow we have:

$$\frac{\partial u}{\partial x} + \frac{\partial w}{\partial z} = s(t) \quad (1)$$

Where, u and w are the velocity components respectively in x and z directions. s(t) is an added mass source term depending on the type wave to be generated.

For monochromatic wave, assuming that the wave is generated at $x = 0$, the free surface elevation function of the time t is given by the following equation:

$$h(t) = \frac{H}{2} \sin(\omega t) \quad (2)$$

With H : wave height; ω : wave frequency depending on the wave period T ($\omega = \frac{2\pi}{T}$).

For solitary wave, assuming that the wave is generated at $x = 0$, the local free surface elevation function of the time t is given by the following equation:

$$h(t) = H \operatorname{sech}^2[k(x_s - Ct)] \quad (3)$$

With $\operatorname{sech}()$ is the hyperbolic secant; H : wave height; C the wave celerity given by :

$$C = \sqrt{gd} \quad (4)$$

The parameter k is given by :

$$k = \sqrt{\frac{3H}{4d^3}} \quad (5)$$

The wavelength of a solitary wave is theoretically infinitely long. However for practical purposes we can define an arbitrarily wavelength as :

$$l = \frac{2P}{k} \quad (6)$$

The apparent wave period is defined as :

$$T = \frac{l}{C} \quad (7)$$

The distance x_s is introduced to make the source function is negligible at initial time :

$$x_s = \frac{4d}{\sqrt{H/d}} \quad (8)$$

This implies that 99 % of solitary mass can be generated by the source function at $t = 0$. According to Lin and Liu (1999), the corresponding mass source term is given by :

$$s(t) = \frac{2C h(t)}{A} \quad (9)$$

With, C the wave celerity and A the area of the source region.

It is noted that the factor “2” in Eq. (9) denoted that the wave energy is transported in both directions from the wave generation line source.

In laminar viscous flow, the dynamic transport equation describing the velocity component in the horizontal direction is:

$$\frac{\partial u}{\partial t} + u \frac{\partial u}{\partial x} + w \frac{\partial u}{\partial z} = -\frac{1}{r} \frac{\partial P}{\partial x} + n \left(\frac{\partial^2 u}{\partial x^2} + \frac{\partial^2 u}{\partial z^2} \right) \quad (10)$$

A dissipation zone is used for damping the wave amplitude at the outlet boundary. In this region, a friction source term is added to the vertical velocity component within the momentum transport equation in the vertical direction:

$$\frac{\partial w}{\partial t} + u \frac{\partial w}{\partial x} + w \frac{\partial w}{\partial z} = -g - \frac{1}{r} \frac{\partial P}{\partial z} + n \left(\frac{\partial^2 w}{\partial x^2} + \frac{\partial^2 w}{\partial z^2} \right) - g w \quad (11)$$

With : P the pressure; ν : kinematic viscosity; ρ : fluid density; g : gravitational acceleration. γ : is a dumped function equals to zero except for the added dissipation zone.

$$g(x) = a x + b \quad (12)$$

Where, $x_s < x < x_e$ (subscripts s, e mean starting and end point of damping zone).

α : is the control parameter

The dumping force in horizontal direction is not considered (in Equation 10) in order to avoid the velocity dumping in the uniform horizontal flow.

The mass source term introduce the following source term in the VOF transport equation,

$$\frac{\partial F}{\partial t} + \frac{\partial}{\partial x}(F u) + \frac{\partial}{\partial z}(F w) = F s \quad (13)$$

A cell with an $F = 0$ refers to an empty cell, the one with $0 < F < 1$ is a surface cell and a cell with $F = 1$ is a water full cell, Hirt and al. (1981).

The wave propagation is considered as a two phases flow involving water phase and air phase. We assume that the sliding between the two phases is negligible and that there is no mass exchange across the interface. Hence, the velocity field at the free surface is continued.

2-2 Boundaries conditions

The following boundaries conditions are considered along with these transport equations:

- For the free surface boundary condition, the normal stress is imposed by setting the pressure P equal to the atmospheric pressure P_{atm} ($P = P_{atm}$).
- For open boundary condition, a dissipation zone is added in order to avoid wave reflection at each end. Within such zone it is advantageous to consider in addition to the dumping friction force, a numerical dissipation by applying a coarse grids in the dissipation zones.

The Neumann boundary condition is specified at the end of each dissipation zone.

The initial condition considered is a still water with no wave or current motion.

The PHOENICS (Parabolic Hyperbolic Or Elliptic Numerical Integration Code Series) code, is well suited for the implementation of the above models (Eqns 1 to 8). Within this code the flow velocity and free surface evolution are determined by the finite volume solution (Patankar, 1980). The Van Leer scheme with Total Variation Diminishing (TDV) approach is adopted in order to overcome the discontinuities of flow variables at the interface.

3- Simulations Results

3-1 Regular wave

The computational domain consists of an inner domain of $L_1 = 6$ m, and two sponge layers with a thickness of $S = 5$ m at the outside boundaries (figure 1). The length L_2 of the source region is taken 5% of the incident wavelength. The absorption function is linearly decreasing in the horizontal direction.

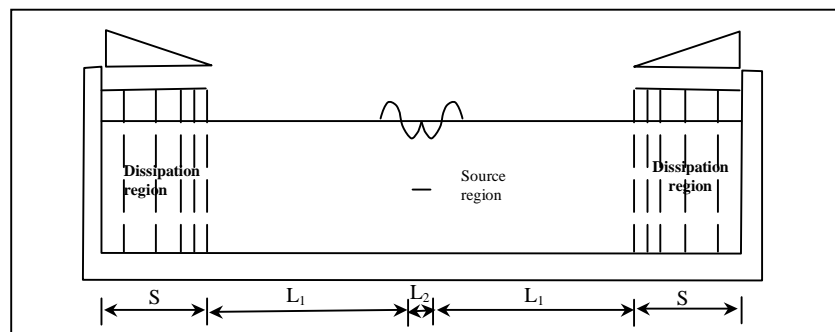


Figure 1 : Computational domain for generating monochromatic incident wave.

The still water depth at the channel is $d = 0.2\text{m}$. The incident wave have the following characteristics : $H = 0.01\text{ m}$, $T = 1\text{ s}$, $d = 0.2\text{ m}$, $C = 1.21\text{ m/s}$, $k d = 1.04$ (k is the wave number).

A uniform mesh size in x direction is used : $\Delta x = \lambda/34$. In the vertical direction a non uniform mesh is considered with minimum $\Delta z = H/25$ around the free surface. For this linear wave, a time step of $\Delta t = T/60$ is used.

Figure 2 shows the free surface elevation at $t = 4 T$ and $t = 6T$, along the wave tanks. The generated unidirectional monochromatic wave profiles are accurately reproduced compared to linear wave theory (Bonnefille, 1992). Both wave amplitudes and wavelengths are almost equal to the incident values. Also, wave energy is dissipated at the sponge layer almost perfectly.

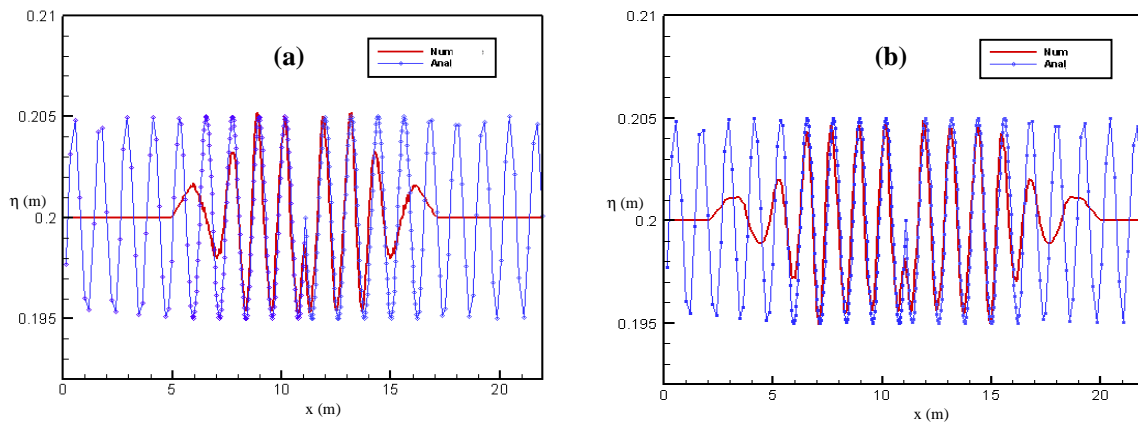
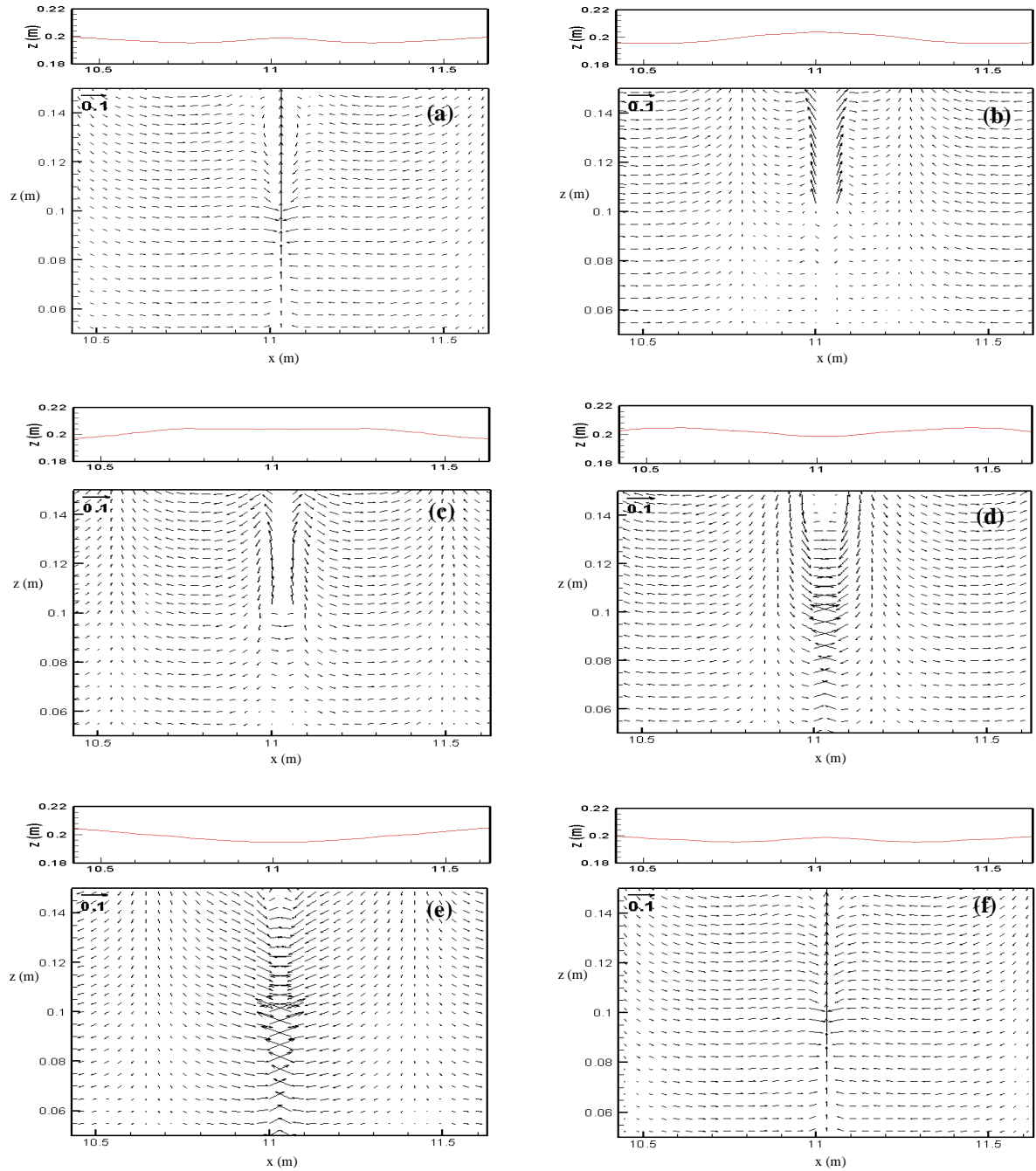


Figure 2 : Comparison between numerical free surface elevation and analytical results a) $t = 4.0 T$; b) $t = 6.0 T$.

In order to explain the wave generation mechanism with internal mass source we represented in figure 3-a to f, the velocity field and free surface profile around source region during one period. When $t = 3.0 T$ and $t = 4.0 T$, figure 3 a) and f), $s(t) = 0$ and the velocity divergence is equal to zero. Hence, the velocity field is almost identical to linear theory except in the center of the source region where the computed velocity has no physical meaning.

At $t = 3.2 T$, figure 3 b), we have an upward motion of the free surface associated to the increase of mass source. The added mass produce the desired free surface shape because the length L_3 of the source region is very narrow ($L_2 = 5\% \lambda$) as shown in figure 3 c).

From $t = 3.6 T$ to $4.0 T$, figure 3 d-e), the mass source decreases, and the free surface is sucked into the source region which induces returning flow. We note that since the incident wave is periodic, the velocity and free surface are almost identical at $t = 3.0 T$ and $t = 4.0 T$.



**Figure 3 : Numerical free surface elevation and velocity field around source region at :
a) $t = 3.0 T$; b) $t = 3.2 T$; c) $t = 3.4 T$; d) $t = 3.6 T$; e) $t = 3.8 T$; f) $t = 4.0 T$.**

Fig 4 shows the free surface and velocity field under a sinusoidal wave along one wavelength at time $t = 5 T$. The direction of wave propagation is from left to right; under the crest the fluid velocity is also in that direction. However, under the trough the velocity is in the negative x direction.

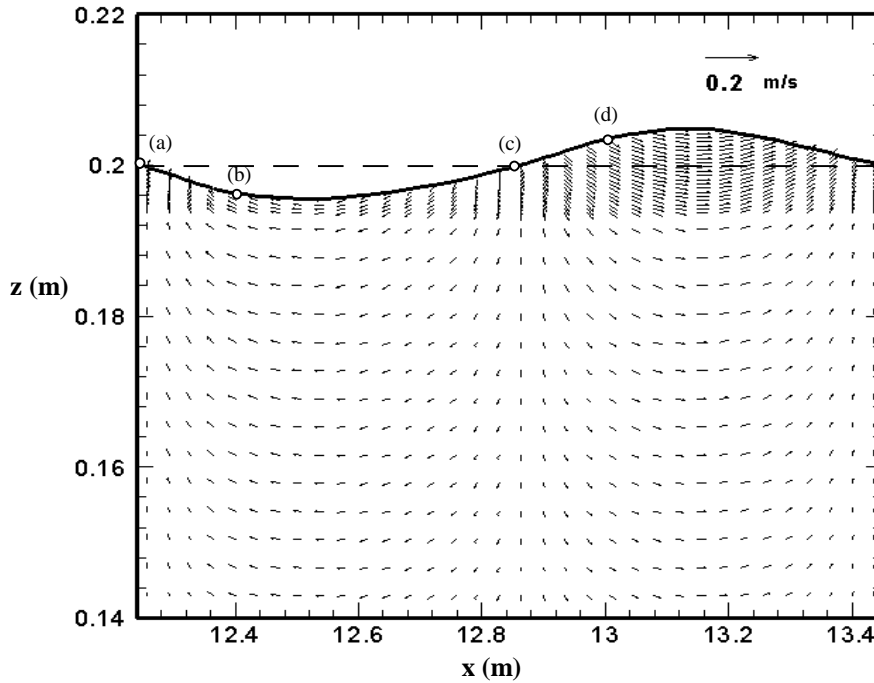
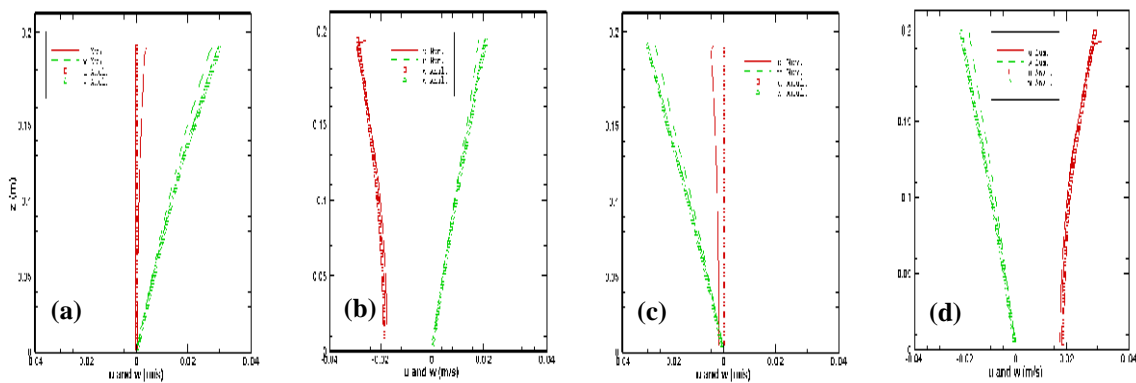


Figure 4 : Numerical free surface elevation and velocity field for unit wavelength at $t = 5 T$.

In order to verify the accuracy of the proposed model, the numerical velocity profiles at different locations (a to c shown in fig 4), are compared to the linear theory solutions. The numerical and theoretical results of the vertical distribution of the horizontal and vertical velocity components are represented in Fig 5.



**Figure 5 : Numerical and analytical velocity profiles at different sections :
a) $x = 12.24$ m; b) $x = 12.40$ m; c) $x = 12.85$ m; d) $x = 13.00$ m.**

In the cases where the free surface displacement is equal to zero, the fluid particles moves upward (fig. 5-a). The vertical velocity component decreases exponentially from free surface to the bottom. After 0.13λ (fig. 5-b), the direction of the particles fluid velocity is inclined from the bottom and opposite to the wave propagation direction. After a one half wavelength (fig 5-c), the fluid particles moves downward. This fluid particle displacement is symmetric to that observed in figure 5-a). A symmetric behavior is also observed between figure 5-b) and 5-d) due to linear character of the sinusoidal wave. The comparison shows that

the numerical results follow the linear solution satisfactory except for location c) where small disagreement is observed due to possible small phase error.

3-2 Solitary wave

In order to validate the proposed generation method for nonlinear wave, we consider the propagation, of the solitary wave in constant water depth, $d = 0.20$ m. The offshore incident solitary wave height is $H = 0.01$ m (the ratio of wave height to water depth ratio is $\frac{H}{d} = 0.05$).

The total horizontal length of computational domain is 16.12 m including 6 m for the dissipation zone. The numerical computation is conducted with $NX = 241$ and $NZ = 116$ grids respectively in x and z directions. The finest grid size in horizontal and vertical directions are chosen as $\Delta x = 0.05$ m and $\Delta z = 0.0004$ m, respectively. The time increment is $\Delta t = 0.013$ s. At $t = 2.13$ s (fig 6) we have intercepted the leading and trailing edges of two solitary wave generated by the mass source function.

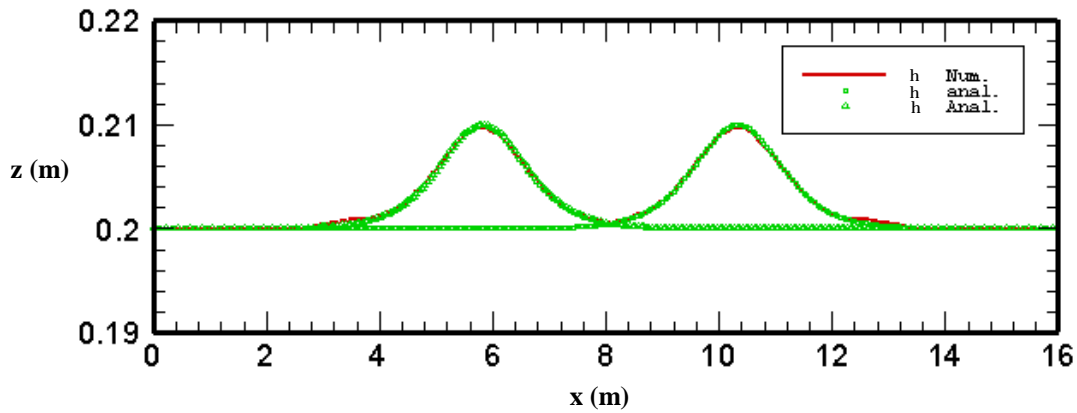


Figure 6 : Numerical and analytical free surface elevation for solitary wave at $t = 2.13$ s.

The numerical free surface profile is accurately reproduced except for the trailing edge where small discrepancy is observed. The numerical free surface and velocity field for this solitary wave is represented in figure 7.

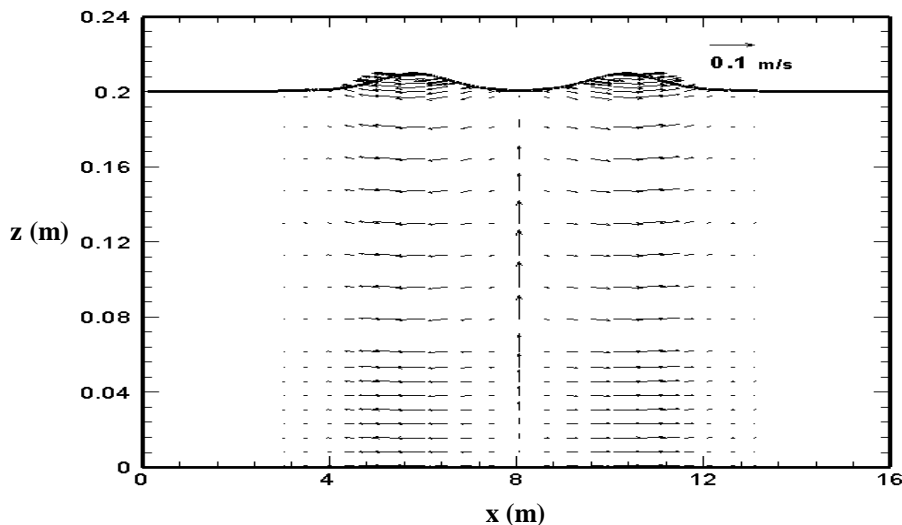


Figure 7 : Numerical free surface elevation and velocity field for solitary wave at $t = 2.13$ s.

The two generated waves is propagating in opposite direction. The direction of the velocity vector at the crest following the direction of propagation. Due to nonlinear character of solitary wave, no symmetric behavior is observed as the sinusoidal wave. We note that the velocity in the vicinity of the source region is always directed upward and has no physical meaning. Fig. 8 shows the evolution of a solitary wave propagating in a channel with constant water depth.

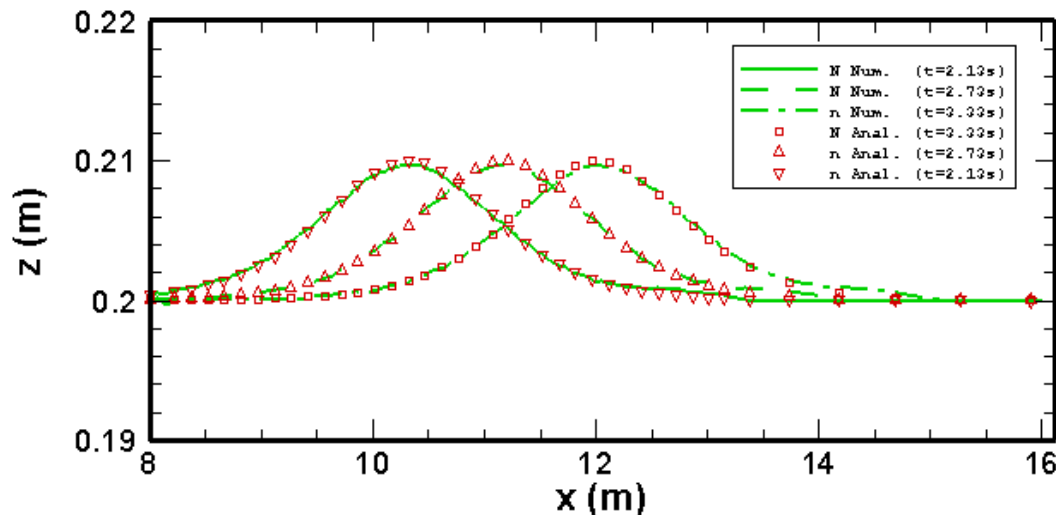


Figure 8 : Numerical and analytical free surface elevation for solitary wave at different times.

The wave preserves the permanent shape and propagates with the same wave velocity. In fact, with the same time interval, the distance traveled by wave is identical.

4- Conclusions

The proposed numerical wave generation model based on an added mass source term in internal flow region was proven to be able to generate small amplitude and solitary waves. For monochromatic wave, the wave profiles and the velocity profiles are similar to those of the analytical solutions. However, Small phase difference in free surface is noted which induce small discrepancy in the horizontal velocity component for one half of the wavelength. The free surface profile, for solitary wave, is also accurately predicted and his permanent shape is preserved during the propagation period.

Based on previous research works from the specialized literature, a wide validation process will be performed to demonstrate the accuracy of the numerical wave generator model. This generation method is also very useful for the practical computation of wave-current interaction wave-structure interaction (wave run-up and wave breaking).

5- References

- [1] Bonnefille R. - Cours d'hydraulique maritime, Masson, 1992.
- [2] Borsen, M. and Larsen, J. - Source generation of nonlinear gravity wave with boundary integral equation method. *Coast. Eng.* **11**, pp. 93–113 (1987).
- [3] Dong C.M. and Huang C.J. - On a 2-D Numerical Wave Tank in Viscous Fluid. *Proceedings of the Eleventh (2001) International Offshore and Polar Engineering Conference Stavanger, Norway, June 17-22, (2001).*

- [4] Grilli, S.T., Guyenne, P. and Dias, F. - A fully nonlinear model for three-dimensional overturning waves over arbitrary bottom. *International Journal for Numerical Methods in Fluids*, 35(7), 829-867 (2001).
- [5] Hirt, C.W. and Nichols, B.D. -. Volume of fluid (VOF) method for the dynamics of free boundaries. *J. Comp. Phys.* 39, pp. 201–225 (1981).
- [6] Kawasaki, K. - Numerical simulation of breaking and post-breaking wave deformation process around a submerged breakwater. *Coast. Eng. J.* 41, pp. 201–223 (1999).
- [7] Larsen, J., Dancy, H. - Open boundaries in short wave simulations : a new approach. *Coastal Eng.* 7, pp 285-297 (1983).
- [8] Lin P. and Liu P. - Internal wave-maker for Navier-Stokes equations models. *Journal of waterway, port, coastal, and ocean engineering.* Vol 125 N° 4, 207-215. July-august (1999).
- [9] Lin Pengzhi, Liu Philip L-F - A numerical study of breaking waves in the surf zone. *Journal of Fluid Mechanics.* Vol 359, 239-264 (1998).
- [10] Patankar S.V. - *Numerical Heat Transfer and Fluid Flow.* McGraw (1980).
- [11] Wei, G., Kirby, J. T., and Sinha, A. - Generation of waves in Boussinesq models using a source function method. *Coastal Eng. J.*, 36, 271-299 (1999).